



Contents lists available at ScienceDirect

Journal of King Saud University – Science

journal homepage: www.sciencedirect.com



Original article

# Biological synthesis and characterization of *Passiflora subpeltata* Ortega aqueous leaf extract in silver nanoparticles and their evaluation of antibacterial, antioxidant, anti-cancer and larvicidal activities

Settu Loganathan<sup>a,b</sup>, Kuppusamy Selvam<sup>a,\*</sup>, Govindaraj Padmavathi<sup>a</sup>, Muthugounder Subramanian Shivakumar<sup>c</sup>, Sengottayan Senthil-Nathan<sup>d</sup>, Arumuga Gounder Sumathi<sup>e</sup>, M. Ajmal Ali<sup>f</sup>, Saeedah M. Almutairi<sup>f</sup>

<sup>a</sup> Department of Botany, Periyar University, Periyar Palkalai Nagar, Salem 636 011, Tamil Nadu, India

<sup>b</sup> Department of Chemical Engineering, Sri Sivasubramaniya Nadar College of Engineering, Kalavakkam 603110, Tamil Nadu, India

<sup>c</sup> Department of Biotechnology, Periyar University, Periyar Palkalai Nagar, Salem 636 011, Tamil Nadu, India

<sup>d</sup> Division of Biopesticide and Environmental Toxicology, Sri Paramakalyani Centre for Excellence and Environmental Sciences, Manonmaniam Sundaranar University, Alwarkurichi, Tamil Nadu 627 412, India

<sup>e</sup> Department of Pathology, Emory University, GA, United States

<sup>f</sup> Department of Botany and Microbiology, College of Science, King Saud University, P.O. 2455, Riyadh 11451, Saudi Arabia

## ARTICLE INFO

### Article history:

Received 6 October 2021

Revised 25 November 2021

Accepted 16 January 2022

Available online 22 January 2022

### Keywords:

Silver Nanoparticles

FE-SEM

H<sub>2</sub>O<sub>2</sub>

Colon cancer

*Cx. quinquefasciatus*

## ABSTRACT

*Passiflora subpeltata* contain rich source of secondary metabolites and its plant materials mostly used for cancer and mosquito related problem. Therefore, in this study, green synthesis of silver nanoparticles using *Passiflora subpeltata* of aqueous extract (*Ps*-AgNPs) as reducing and stabilizing agent. The UV-Visible spectra of *Ps*-AgNPs showed absorption peak at 456 nm and formation of AgNPs. XRD pattern showed the crystalline nature and SEM images displayed predominantly spherical shape of NPs. FT-IR analysis exhibition capping of AgNPs by bioactive compounds from *Ps*-AgNPs. Antibacterial activity in *Ps*-AgNPs shown good activity with best of *B. cereus* (27 mm) at higher dose of 75 µg/mL. Antioxidant activity was tested against DPPH, ABTS and H<sub>2</sub>O<sub>2</sub> assays and the best scavenging assay were observed in DPPH with IC<sub>50</sub> value of 108.92 µg/mL. The anti-proliferative activity in human colon cancer cell-line (HT-29) indicates that the significant result with IC<sub>50</sub> value of 33.05 µg/mL. Larvicidal activity of *Ps*-AgNPs showed good activity against *Cx. quinquefasciatus* larvae (LC<sub>50</sub>-4.99 units and LC<sub>90</sub>-22.19units). The green synthesized NPs could be potential activity and it used in different biomedical application.

© 2022 The Authors. Published by Elsevier B.V. on behalf of King Saud University. This is an open access article under the CC BY-NC-ND license (<http://creativecommons.org/licenses/by-nc-nd/4.0/>).

## 1. Introduction

Nanoparticles stand for a particle with a nano size of 1–100 nm. These materials are latest, unique, and superior physical and chemical properties compared to its massiveness structure, due to an increase in the ratio of the surface area per volume of the material/particle (Aritonang et al., 2019). Hence, the nanoparticles find applications in human life for different fields (Rathnakumar

et al., 2019). The nanoparticles such as gold, silver, titanium and platinum are commonly used in nanoparticle synthesis (Khandel et al., 2018). Metallic NPs, particularly, silver NP's has various therapeutically applications due to low dose have enhanced bioavailability, target specificity and long-lasting activity. The synthesis of metal nanoparticles, can be achieved by various strategies for example, physical, chemical and biological. Among these methods, biological synthesis is fast, low cost, environmental-friendly and hence is a preferred method (Rajkumar et al., 2018). Silver nanoparticles (AgNPs) synthesized using different plants such as *Rumex hastatus* (Gul et al., 2021a,b), *Galphimia glauca* (Chakraborty et al., 2021), *Ixora brachypoda* (Bhat et al., 2021), *Commiphora myrrh* (Alwhibi et al., 2020). The plant derived silver nanoparticles (Ag-NPs) find extensive use in biological field such as antibacterial, anticancer and larvicidal activities (Divya et al., 2018). Mosquitoes are a vector to convey several tropical diseases as malaria, dengue fever, chikungunya, Rift Valley fever, filariasis,

\* Corresponding author.

E-mail addresses: [selsarat@yahoo.com](mailto:selsarat@yahoo.com) (K. Selvam), [senthil@msuniv.ac.in](mailto:senthil@msuniv.ac.in) (S. Senthil-Nathan).

Peer review under responsibility of King Saud University.



Production and hosting by Elsevier

<https://doi.org/10.1016/j.jksus.2022.101846>

1018-3647/© 2022 The Authors. Published by Elsevier B.V. on behalf of King Saud University.

This is an open access article under the CC BY-NC-ND license (<http://creativecommons.org/licenses/by-nc-nd/4.0/>).

West Nile fever and Japanese encephalitis. Understanding the main concepts of plant extracts with AgNPs used in traditional medicine as therapeutic agents can help to identify the novel compounds for treating many diseases (Ashwini and Asha, 2017).

Plants are rich source of secondary metabolites and it used for various therapeutically application (Sowndarya et al., 2017). Nano-based drug delivery systems create a new way in pharmaceutical industry (Patra et al., 2018). Plant metabolites with metal nanoparticles combination could be capable of deliver the drugs. *Passiflora subpeltata* Ortega belongs to the Passifloraceae (Passion flower family) and its commonly known as “passion flower” as well as malaikovai (tamil name). It distributed in some Pacific islands. *Ps* plants an exotic fast-growing vine plant with two–three ornate flowers contain yellow–green fruits. Traditionally, the plant is utilized for its properties such antioxidant, analgesic, anti-inflammatory, antipyretic, anti-proliferative etc., (Chunchegowda et al., 2020). In the current work low cost synthesis of AgNPs by a one-step reduction of silver ions using *Passiflora subpeltata* leaf extract was done to assess the nanoparticles synthesis. The physicochemical characteristics of the synthesized silver nanoparticles were analyzed using various techniques (UV–vis, FT-IR, FE-SEM with EDAX and XRD analysis). The antibacterial, antioxidant, anti-proliferative and larvicidal activities of the synthesized *Ps*-AgNPs were estimated.

## 2. Materials and methods

### 2.1. Collection and extraction

*P. subpeltata* was collected from Shevaroy hills (August-2019) in Salem district, Tamil Nadu, India. *Ps*-leaves were dried for two weeks and it's powdered using steel blender. The powder of the plant leaves was weighed at 10 g and transfer into beaker (100 mL-D-H<sub>2</sub>O) than boiled in 30 min. The filter paper (Whatman no. 1) was used to filter the extract and the solutions were refrigerated (4 °C) for further study.

### 2.2. Synthesis of AgNPs

About 10 mL of *Ps*-aqueous leaf extract (ALE) was added into 90 mL of silver nitrate (Mercury Scientific, Salem) solution at room temperature and allowed them to mix properly. As a control AgNO<sub>3</sub> was used. After, 24 h, the mix elucidation changed from yellow to dark brown colour. The solution was centrifuged at 5000 rpm (560 g force) for 12 min and the pellet was obtained. The pellets were washing out double distilled water than dried and analyzed.

### 2.3. Characterization of AgNPs

*Ps*-AgNPs in reduction was observed using UV–Vis spectroscopy (Shimadzu UV-1800) in the range of 400 to 700 nm wavelength. Crystalline property was analyzed by the X-Ray Diffraction (Rigaku Mini Flex,) operating at 40 kV with 30 mA using CuK $\alpha$  ( $\lambda = 0.154 \text{ \AA}$ ) radiation with the crystallite sizes of silver nanoparticles and were calculated by the equation of Debye-Scherrer formula. Functional groups were analyzed through FT-IR (Perkin Elmer-Tensor 27, Bruker, Germany) and wavelength of 400–4000 cm<sup>-1</sup>. Scanning electron microscopy (FE-SEM-EVO 18, ZEISS, UK) was used in shape and size were analyzing for NPs with elemental was analyzed (EDAX-Quorum Technologies, U.K).

### 2.4. Antioxidant assay

#### 2.4.1. 2,2-Diphenyl-1-picrylhydrazyl assay (DPPH)

DPPH radical scavenging activity of *Ps*-AgNPs was described by earlier, Loganathan et al. (2021a,b). In briefly, 1.0 mL of DPPH solu-

tion (0.2 mM) was taken having sample various dose (20, 40, 60, 80, and 100  $\mu\text{g/mL}$ ) were used and stand for 30 min beneath dark conditions. After 30 min the absorbance was read at 517 nm (UV–visible Spectrophotometer). Ascorbic acid was used as control. The percentage of inhibition in DPPH radical scavenging activity was calculated as follows;

$$\text{DPPH scavenging effect (\%)} = \frac{A_0 - A_1}{A_0} \times 100$$

$A_0$ -Control,  $A_1$ -AgNPs.

#### 2.4.2. Hydroxyl scavenging

The assay was described by earlier, Loganathan et al. (2021a,b). 1 mL of various concentration of sample (20–100  $\mu\text{g/mL}$ ) was mixed into 3 mL H<sub>2</sub>O<sub>2</sub> (1.0 mL of 1.5 mM FeSO<sub>4</sub>, 0.7 mL of 6 mM H<sub>2</sub>O<sub>2</sub>, 0.3 mL of 20 mM sodium salicylate). The reaction mixture was incubated for 37 °C and the absorbance was measured at 562 nm. The percentage scavenging effect was calculated as,

$$\text{Scavenging activity} = \left[ 1 - \frac{(A_1 - A_2)}{A_0} \right] \times 100$$

Where,  $A_0$ -control,  $A_1$ -sample and  $A_2$ -absorbance without sodium salicylate.

#### 2.4.3. 2,2'-Azino-bis-3-ethylbenzothiazoline-6-Sulfonic acid (ABTS)

This assay was followed by, Loganathan et al. (2021a,b). The reaction was began via the addition of 1.0 mL of diluted ABTS to 10  $\mu\text{L}$  of different concentrations (20, 40, 60, 80 and 100  $\mu\text{g/mL}$ ) of sample and also 10  $\mu\text{L}$  of ethanol as a control. The absorbance was read at 734 nm after 6 min and the percentage inhibitions were calculated. The inhibition was calculated according to the equation;

$$\text{IC (\%)} = \frac{A_0 - A_1}{A_0} \times 100$$

Where,  $A_0$  is absorbance of control reaction,  $A_1$  is absorbance of AgNPs.

### 2.5. Antibacterial activity

The antibacterial efficacy of AgNPs was examined by the agar well diffusion method (Anonymous, 1996). The selected human pathogens like as, *Bacillus cereus* and *Escherichia coli* were obtained from Department of Microbiology, Periyar University, Salem. They were maintained in nutrient agar slants as well as sub-cultured from time to time in the laboratory. The inoculums were prepared by growing a single colony for overnight in nutrient broth and by adjusting the turbidity to 0.5 McFarland standards Kora et al., (2009). *B. cereus* and *E. coli* were tested using of *Ps*-AgNPs. The test cultures were swabbed on nutrient agar (NA) Plates and permissible to dry for 10 min. A total of three concentrations used like as 25, 50 and 75  $\mu\text{g}$ . Chloramphenicol was used as positive controls (30  $\mu\text{g/disc}$ ). The culture plates were incubated for 12 h at 37 °C. Inhibition zones were measured in millimeters (mm).

### 2.6. Anti-proliferative activity

#### 2.6.1. Cell culture

Colon cancer cell line (HT-29) was obtained from National Centre for Cell Science. The cell lines were grown in Dulbecco with modified eagle medium (DMEM) elevated glucose medium (Sigma Aldrich, USA), as increase with 10% fetal bovine serum, as well as antibiotics (20 mL of penicillin) (Hi Media, India). This cell line was kept in culture at 37 °C and 5% of humidified CO<sub>2</sub> atmosphere.

#### 2.6.2. Cell treatment procedure

This assay was followed by earlier, Mosmann, (1983). The monolayer cells were detached with trypsin-ethylene diamine

tetra acetic acid (EDTA) to make single cell suspensions and viable cells were counted using a hemocytometer and diluted with medium containing 5% FBS to give final density of  $1 \times 10^5$  cells/mL. One hundred microlitres per well of cell suspension were seeded into 96-well plates at plating density of 10,000 cells/well and incubated to allow for cell attachment at 37 °C, 5% CO<sub>2</sub>, 95% air and 100% relative humidity. After 24 h the cells were treated with serial concentrations of the Ps-AgNPs. They were initially dissolved in dimethylsulfoxide (DMSO) and an aliquot of the sample solution was diluted to twice the desired final maximum test concentration with serum free medium. Additional four serial dilutions were made to provide a total of five concentrations of AgNPs (6.5, 12.5, 25, 50 and 100 µg/mL). Aliquots of 100 µl of these different sample dilutions were added to the appropriate wells already containing 100 µl of medium, resulting in the required final sample concentrations. Following sample addition, the plates were incubated for an additional 48 h at 37 °C, 5% CO<sub>2</sub>, 95% air and 100% relative humidity. The medium containing without samples were served as control and triplicate was maintained for all concentrations.

### 2.6.3. MTT assay

3-[4,5-Dimethylthiazol-2-yl] 2,5-diphenyltetrazolium bromide (MTT) is a yellow water soluble tetrazolium salt. A mitochondrial enzyme in living cells, succinate-dehydrogenase, cleaves the tetrazolium ring, converting the MTT to an insoluble purple formazan. Therefore, the amount of formazan produced is directly proportional to the number of viable cells. After 48 h of incubation, 15 µl of MTT (5 mg/ml) in phosphate buffered saline (PBS) was added to each well and incubated at 37 °C for 4 h. The medium with MTT was then flicked off and the formed formazan crystals were solubilized in 100 µl of DMSO and then measured the absorbance at 570 nm using micro plate reader. Cell morphology was taken from Confocal microscope (Olympus, Japan). The living cells percentage was calculated below.

$$\text{Cell viability(\%)} = \frac{\text{OD of Test (NPs)}}{\text{OD of Control(Untreated)}} \times 100$$

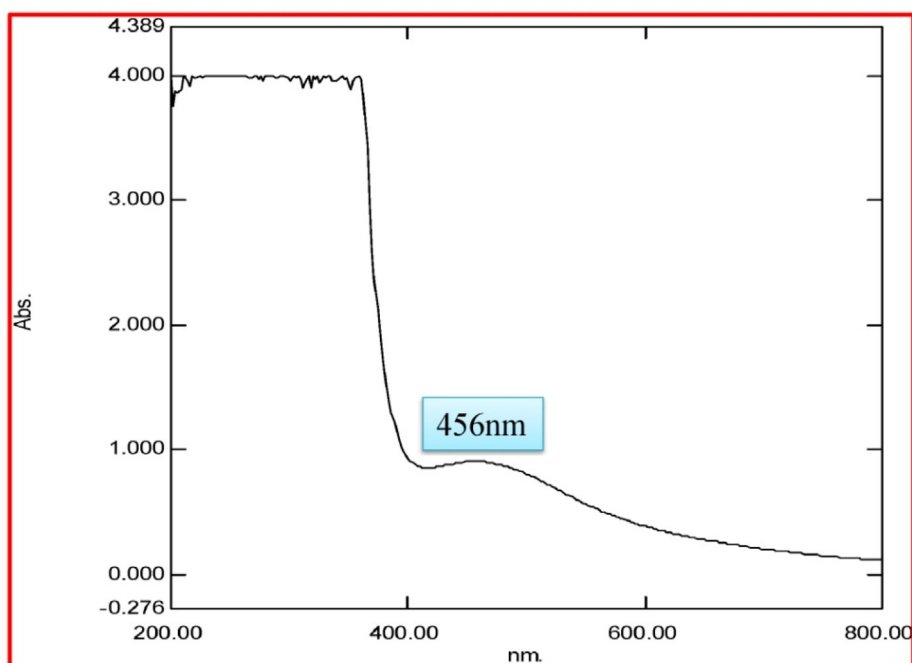


Fig. 1. UV-visible absorbance spectra obtained from silver nanoparticles using *P. subpeltata* aqueous leaf extracts (Ps-ALE).

## 2.7. Larvicidal activity

### 2.7.1. Collection and rearing of mosquito larvae

*Ae. aegypti*, *An. stephensi* and *Cx. Quinquefasciatus* were collected from Indian Council of Medical Research (ICMR)-Vector Control Research Centre, Madurai and then it kept during 14:10 h photoperiod, 27 °C, 70 ± 5%- Relative Humidity (RH) with provided the fed.

### 2.7.2. Larvicidal bioassay

Bio-efficacy was performed as per method of WHO (2005) standard with several changes as per the protocol of Thandapani et al. (2018). Larvae of 4th instar in 20 number were added each plastic cup (200 mL - D.H<sub>2</sub>O). Ps-ALE and Ps-AgNPs concentrations such as, 5, 10, 15, 20 and 25 mg/L were supplemented to the cups. The control treatment was also maintained (distilled water). Larval death was counted after 12 and 24 h. Mortality percentage (larvae) was labeled to average of three replicates. In earlier, method of Abbott, (1925) was used for calculated in larval mortality and death.

## 2.8. Statistical analysis

The results were analyzed a Mean ± SD. Biological activity data was subjected to One and Two-Way ANOVA, with Dunnett's Multiple Comparison tests using PRISM software version 5.2 (Graph Pad Software Inc, USA). The larval mortality was calculated by Probit analysis for finding out LC<sub>50</sub>, and LC<sub>90</sub> values. The chi square values were also calculated by SPSS software version 20.0 (SPSS., USA).

## 3. Results and discussion

### 3.1. UV-Vis spectra analysis

Ps-AgNPs in UV absorption peak at wavelength of 456 nm (Fig. 1). The same results were reported by Patra et al. (2019). The Surface Plasmon Resonance (SPR) is a confirmation of the synthesis of Ps-AgNPs. In recent report, AgNPs in *Garcinia kola* was showed UV absorbance peak at 445 nm (Akintelu et al., 2021). Mtambo et al. (2019) was studied the *Bidens pilosa* extract of AgNPs showed uv absorption peak at 410 nm.

### 3.2. FT-IR study

Ps-AgNPs of FT-IR spectra shown in Fig. 2. The intense peaks range at  $1050\text{ cm}^{-1}$  for S=O (sulfoxides),  $1347.41\text{ cm}^{-1}$  for C-X (Fluoride),  $1605.44\text{ cm}^{-1}$  for N-H (amines and amides)  $2836.42\text{ cm}^{-1}$  for C-H (Aldehyde) and  $3078.00\text{ cm}^{-1}$  for C-H (Alkenes) are represented in Table 1. The essential functional groups such as, alcohol, amides, alkanes, methyl, aliphatic and halides confirmed their presence of NPs. It was stabilizing, capping and dipping agents of the AgNPs (Vijayaraghavan et al., 2012). Gul et al. (2021a,b) have reported that the *Rumex hastatus* derived AgNPs showed the presence of various functional groups. *Malva verticillata* extracts of AgNPs displayed the presence of different bioactive compounds (Sk et al., 2020).

### 3.3. XRD

XRD results from Ps-AgNPs shown 9 peaks at  $2\theta$  ranges of  $27.87^\circ$ ,  $32.14^\circ$ ,  $38.77^\circ$ ,  $44.20^\circ$ ,  $46.10^\circ$ ,  $54.40^\circ$ ,  $57.34^\circ$ ,  $64.34^\circ$  and  $77.72^\circ$  can be corresponds values to 210, 101, 111, 200, 231, 142, 241, 220 and 311 are displayed in Fig. 3. In, similar result was finding in AgNPs of *Sargassum myriocystum* (Balaraman et al., 2020). *Asphodelus aestivus* aerial part extract of AgNPs displayed presence of four diffraction values (Fafal et al., 2017). The lattice planes of pure silver based on the face-centre cubic structure (JCPDS No. 4-0783) and the XRD results was clearly indicate that the crystalline in nature of AgNPs. In earlier report, the AgNPs from *Carmona retusa* leaf extract showed 4 diffraction peaks by XRD (Rajkumar et al., 2018). In this study, the average crystal size of nanoparticles measure by Debye Scherrer's formula and its size of 22.6 nm.

**Table 1**

FT-IR analysis of AgNPs using *P. subpeltata* aqueous leaf extract (Ps-ALE).

Wave number ( $\text{cm}^{-1}$ )	Intensity	Group Compound	Functional group
1050.47/Bending	Strong	S=O	Sulfoxides
1347.41/Stretch	Strong	C-X	Fluoride
1605.44/Bending	Medium-	N-H	Primary and secondary
2836.42/Stretch	Strong	C-H	amines and amides
3078.00/Stretch	Weak	C-H	Aldehyde
	Medium		Alkenes

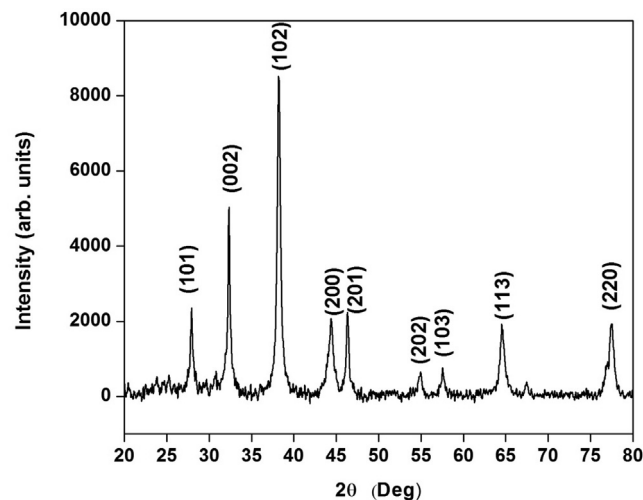


**Fig. 3.** XRD pattern of silver nanoparticles synthesized in *P. subpeltata* aqueous leaf extracts (Ps-ALE).

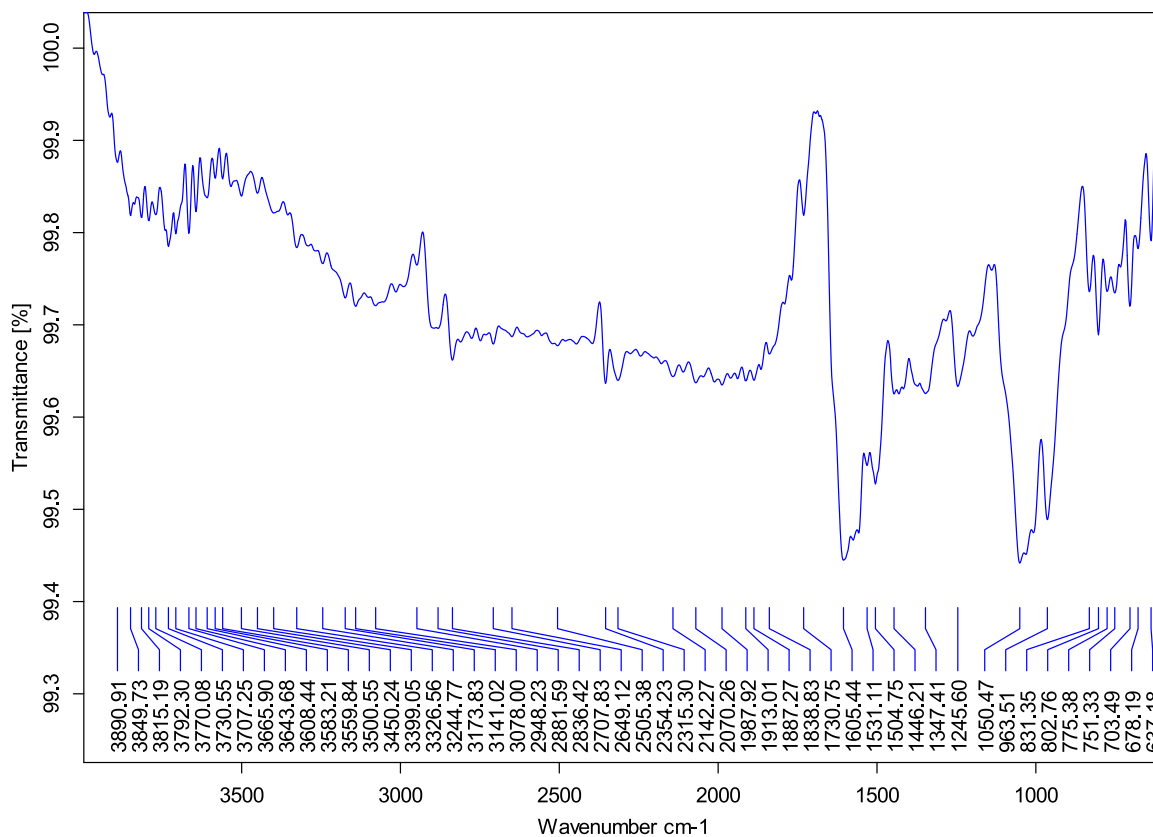


**Fig. 2.** FT-IR studied from silver nanoparticles synthesized in *P. subpeltata* aqueous leaf extracts (Ps-ALE).

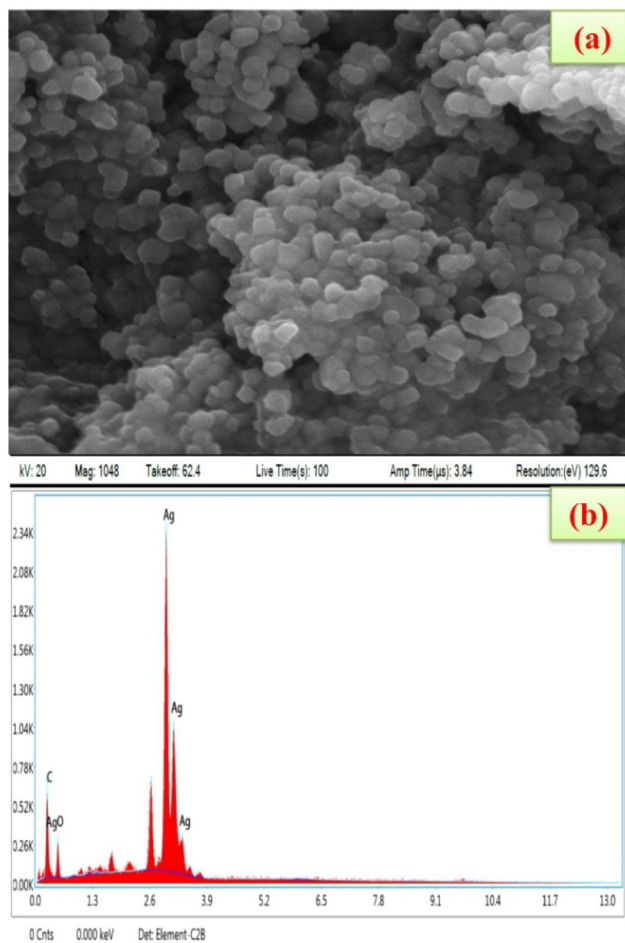


**Fig. 4.** (a) Scanning Electron Microscope image of silver nanoparticles synthesized in *P. subpeltata* aqueous leaf extracts (Ps-ALE), (b) Edax spectrum showed the presence of strong Ag signals.

### 3.4. FE-SEM

Ps-AgNPs nanoparticles morphological structure in spherical with size ranging between 20 and 40 nm (Fig. 4a). Similarly were observed from, AgNPs of *Ajug abracteosa*; *Cinnamomum tamala* (Afreen et al., 2020; Nahar et al., 2020). EDAX spectra indicated that the strong Ag signal and other elemental such as Carbon and Silver oxide (Fig. 4b). Huong and Nguyen (2021) have analysed the AgNPs by *Brassica oleracea* leaves extract of EDAX spectrum showed the presence of Ag (Senthil-Nathan, 2013,2015, 2020).

### 3.5. Antibacterial potential

Fig. 5 displayed the potential antibacterial activity in Ps-AgNPs. The high level zone of inhibition were recorded in *B. cereus* (27.5 mm) and *E. coli* (23.0 mm) at 75  $\mu\text{g/mL}$  (Table 2). Biosynthesized in CuO-NPs contain good activity in lower concentrations (Kasi et al., 2021). Gul et al. (2021a,b) have stated that the *Rumex hastatus* derived AgNPs showed promising activities. The three most common mechanisms proposed to date are (1) the disruption of ATP production and DNA replication by uptake of free silver ions, (2) ROS generation by silver and silver nanoparticles and (3) direct damage of silver nanoparticles to the cell membranes (Marambio-Jones and Hoek, 2010). The study indicated that the AgNPs were acted efficiently against the tested microbes and than it used for another source of antibiotics.

### 3.6. Antioxidant activity

The scavenging ability of Ps-AgNPs was determined using DPPH, ABTS and  $\text{H}_2\text{O}_2$ . DPPH assay, the highest percentage of inhibition was seen in 55.30 at 125  $\mu\text{g/mL}$ . The percentage of inhibition was increased with increasing the concentration of the sample (F-16.12;  $df=4$ ;  $P < 0.01$ ,  $P < 0.001$ ) (Fig. 6(a)). Similar report were obtained from, AgNPs in stem bark extract of *Diospyros montana* (Bharathi et al., 2018). DPPH- $\text{IC}_{50}$  value of Ps-AgNPs was found to be 108.92  $\mu\text{g/mL}$  while  $\text{IC}_{50}$  values for standard (ascorbic acid)

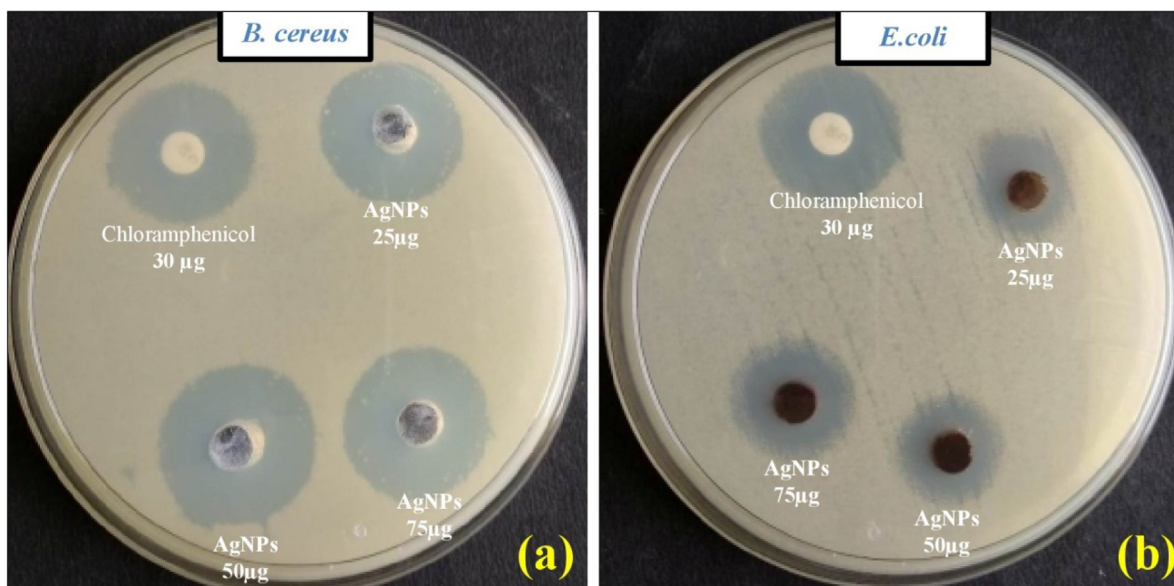


**Fig. 5.** Antibacterial study of silver nanoparticles synthesized in *P. subpeltata* aqueous leaf extracts (Ps-ALE), (a) *B. cereus*, (b) *E. coli*.

**Table 2**  
Antibacterial activity of AgNPs using *P. subpeltata* aqueous leaf extract (*Ps*-ALE).

Microorganisms	Zone of inhibition (mm)		
	Positive Control (Chloramphenicol)	25 (µg/mL)	AgNPs 50 (µg/mL)      75 (µg/mL)
<i>B. cereus</i>	29.0 ± 1.5	22.5 ± 1.1	24.5 ± 0.5      27.0 ± 1.1
<i>E. coli</i>	25.5 ± 0.5	17.5 ± 0.5	21.0 ± 1.1      23.0 ± 1.0

Value are given as Data (Mean ± SD) (n = 3) represent the zone of bacterial growth inhibition (mm).

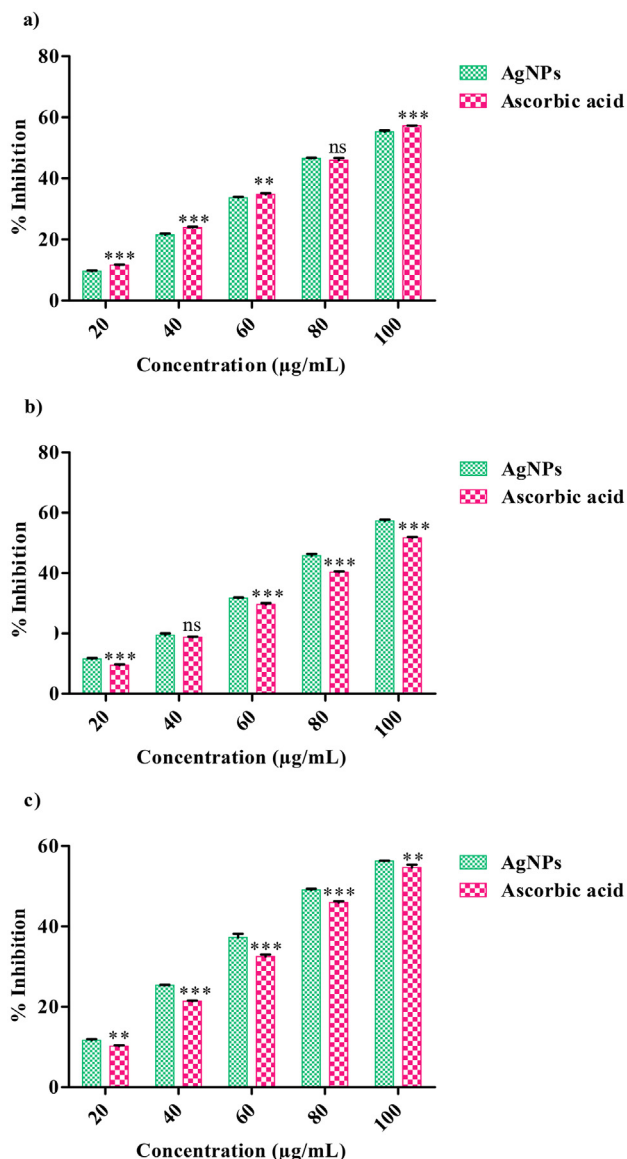


**Fig. 6.** Antioxidant activity of AgNPs using *P. subpeltata* aqueous leaf extract (*Ps*-ALE), (a) DPPH radical scavenging activity, The values are expressed as mean ± SD values and analyzed by Two-Way analysis of variance (ANOVA), Not Significant (ns), Asterisk (\*, \*\*, \*\*\*) indicates significant different among treatments with respect to control ( $P < 0.01$  and  $P < 0.001$ ). (b) ABTS radical scavenging activity, The values are expressed as mean ± SD and analyzed by Two-Way analysis of variance (ANOVA), Not Significant (ns), Asterisk (\*\*\*), indicates significant different among treatments with respect to control ( $P < 0.001$ ). (c) Hydroxyl scavenging activity, The values are expressed as mean ± SD and analyzed by Two-Way analysis of variance (ANOVA), Asterisk (\*, \*\*, \*\*\*) indicates significant different among treatments with respect to control ( $P < 0.01$  and  $P < 0.001$ ).

108.60 µg/mL. In earlier studied from, AgNPs in *Erythrina suberosa* leaf extract showed the DPPH good activity with IC<sub>50</sub> value of 30.04 µg/mL (Mohanta et al. (2017)). The ABTS of *Ps*-AgNPs were displayed the standard (ascorbic acid) IC<sub>50</sub>value of 102.39 µg/mL and also 109.94 µg/mL where estimated by *Ps*-AgNPs (F-47.53; df-4;  $P < 0.001$ ) (Fig. 6(b)). In earlier report, the IC<sub>50</sub>value of 78.10 µg/mL was obtained to *Cassia angustifolia* flower extract of AgNPs (Bharathi and Bhuvaneshwari, 2019). In recent study, green synthesis of AgNPs using various plants extract showed the significant ABTS activities (Viskeliš et al. 2021). The H<sub>2</sub>O<sub>2</sub> of *Ps*-AgNPs and ascorbic acid displayed the scavenging percentage of 57.30% as well as 51.69% at higher dose of 125 µg/mL with IC<sub>50</sub> value of *Ps*-AgNPs as well as standard (ascorbic acid) 121.35; 108.57 µg/mL (F-16.11; df-4;  $P < 0.001$ ). (Fig. 6c). Guntur et al. (2018) were reported that the silver NPs synthesis of *Desmostachhya bipinnata* leaf extract showed the good activity with IC<sub>50</sub> assessment of 259.14 µg/mL. In another report, AgNPs in *Carmona retusa* leaf extract were showed the H<sub>2</sub>O<sub>2</sub> IC<sub>50</sub> value of 47 µg/mL. The antioxidant results indicate that the usage of *Ps*-AgNPs as having antioxidant toward protect health against oxidative stresses with degenerative sicknesses.

3.7. Anti-cancer study

In this study, *Ps*-AgNPs were examined in Human colon cancer cell-line (HT-29) by MTT assay at 24 h. The cell inhibition percentages as well as treated images are displayed in (F-12.27; df-5;  $P < 0.001$ ) Figs. 7 and 8. In this study, was dose depended activity

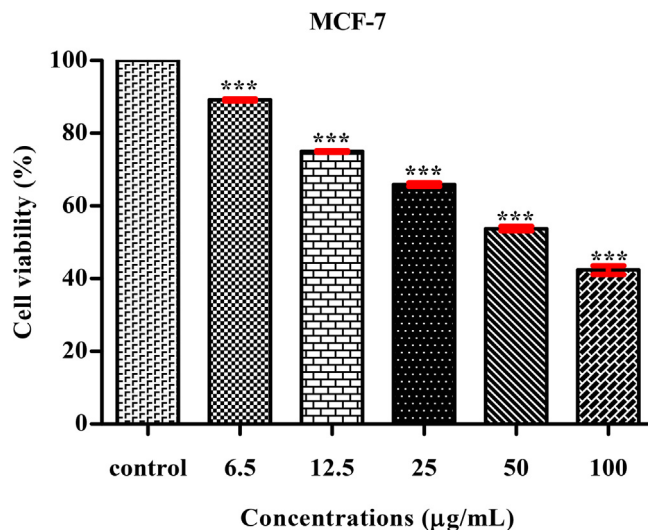


**Fig. 7.** MTT assay confirming the anti-cancer activity of *Ps*-AgNPs against HT-29 cell line, The values are expressed as mean ± SD values and analyzed by One-Way analysis of variance (ANOVA), Asterisk (\*\*\*), indicates significant different among treatments with respect to control ( $P < 0.001$ ).

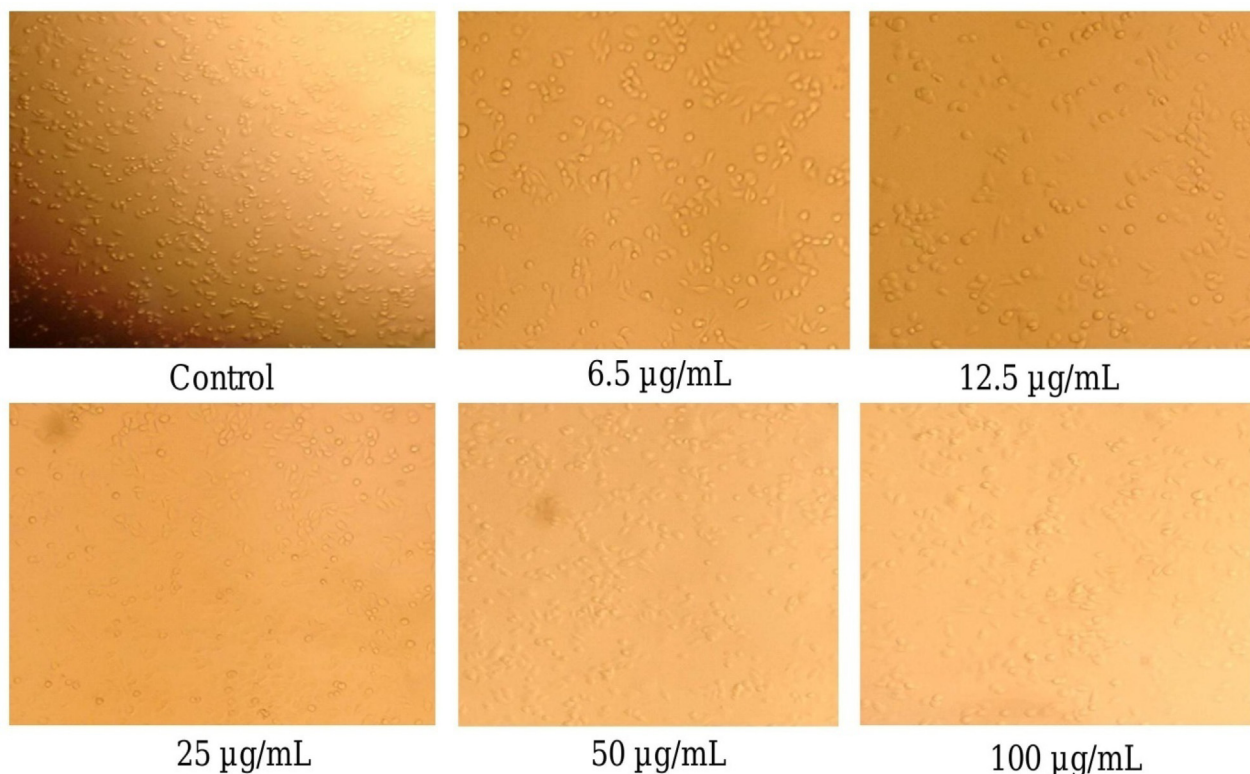


**Fig. 8.** Anti-cancer observed from colon cancer cell line (HT-29) in confocal microscope (340 pixel); Control and various concentrations (6.5, 12.5, 25, 50 and 100 µg/mL) of AgNPs using *P. subpeltata* aqueous leaf extract (Ps-ALE).

**Table 3**  
Larvicidal potential of *P. subpeltata* aqueous leaves extract and Ps-AgNPs against *Aedes aegypti*.

Time (Hour)	Samples	LC <sub>50</sub> (mg/mL) (LCL-UCL)	LC <sub>90</sub> (mg/mL) (LCL-UCL)	χ <sup>2</sup>	Df
12	Plant extract	25.68(22.21–32.45)	47.23(38.32–67.07)	2.35	13
	AgNPs	20.88(19.30–28.11)	46.31(36.21–68.15)	1.87	13
24	Plant extract	13.88(11.72–15.87)	30.72(26.76–37.58)	1.28	13
	AgNPs	10.25(07.67–12.19)	25.94(22.81–31.12)	1.05	13

LC<sub>50</sub>-Lethal concentration kills 50% of the exposed larvae, LC<sub>90</sub>-Lethal concentration kills 90% of the exposed larvae. LCL-Lower confidence limit, UCL- Upper confidence limit, χ<sup>2</sup> Chi-square value, df = degrees of freedom.

**Table 4**  
Larvicidal potential of *P. subpeltata* aqueous leaves extract and Ps-AgNPs against *Anopheles stephensi*.

Time (Hour)	Samples	LC <sub>50</sub> (mg/mL) (LCL-UCL)	LC <sub>90</sub> (mg/mL) (LCL-UCL)	χ <sup>2</sup>	Df
12	Plant extract	27.61(23.68–35.80)	49.31 (39.65–71.59)	2.59	13
	AgNPs	23.40(19.98–30.17)	48.45 (38. 42–72.81)	2.41	13
24	Plant extract	15.43(13.31–17.59)	33.02 (28.53–41.03)	2.89	13
	AgNPs	11.55(08.99–13.58)	28.66 (24.95–35.11)	2.08	13

LC<sub>50</sub>-Lethal concentration kills 50% of the exposed larvae, LC<sub>90</sub>-Lethal concentration kills 90% of the exposed larvae. LCL-Lower confidence limit, UCL-Upper confidence limit, χ<sup>2</sup> Chi-square value, df = degrees of freedom.

(HT-29). Similar observations were studied from *Murraya koenigii* leaf extract of Ag nanoparticles (Roshni et al., 2018). Ps-AgNPs IC<sub>50</sub> value was obtained and it found to be 33.05 µg/mL when the results was compare to earlier report the cytotoxicity studied against HT-29 showed the IC<sub>50</sub> value of 150.8 µg/mL by AgNPs (Venjatadri et al., 2020). Dehghanizade et al. (2018) have exerted that the AgNPs from *Anthemisa tropatana* leaves extract shown better activity against HT-29 with IC<sub>50</sub> value of 4.88 µg/mL.

### 3.8. Larvicidal activity

*P. subpeltata* aqueous leaf extract and AgNPs showed strong larvicidal potential are represented in Tables 3–5. In this study, 100% mortality of larva was identified for *Cx. quinquefasciatus* by Ps-AgNPs. The same work where studied from plant mediated from AgNPs have declared the better larvicidal activity (Sultana et al., 2020; Rajkumar et al., 2019). ZnO-NPs of *K. sumatrensis* shown bet-

**Table 5**  
Larvicidal potential of *P. subpeltata* aqueous leaves extract and *Ps*-AgNPs against *Cx. quinquefasciatus*.

Time (Hour)	Samples	LC <sub>50</sub> (mg/mL) (LCL-UCL)	LC <sub>90</sub> (mg/mL) (LCL-UCL)	χ <sup>2</sup>	Df
12	Plant extract	20.04 (17.58–23.69)	40.45 (33.76–53.89)	1.12	13
	AgNPs	15.60 (13.05–18.31)	37.06 (30.92–49.55)	1.04	13
24	Plant extract	08.45 (4.11–11.12)	29.31 (24.79–38.27)	1.39	13
	AgNPs	04.99 (1.26–7.78)	22.19 (19.21–27.38)	2.05	13

LC<sub>50</sub>-Lethal concentration kills 50% of the exposed larvae, LC<sub>90</sub>-Lethal concentration kills 90% of the exposed larvae. LCL-Lower confidence limit, UCL-Upper confidence limit, χ<sup>2</sup> Chi-square value, df = degrees of freedom.

ter activity with LC<sub>50</sub> 0.08, mg/mL and LC<sub>90</sub> 19.46 mg/mL against *Cx. quinquefasciatus* (Loganathan et al., 2021a,b). Loganathan et al. (2021a,b) reported that the *Knoxia sumatrensis* of the methanolic extract shown strong larvicidal activity on 3 mosquito species with highest toxicity on *Cx. quinquefasciatus* larvae with LC<sub>50</sub> 4.84 mg/mL and LC<sub>90</sub> 19.33 mg/mL. The plant mediated AgNPs has effectively controlled the fourth instar larvae of *Cx. quinquefasciatus*.

#### 4. Conclusion

AgNPs from *Passiflora subpeltata* was successfully synthesized and characterized. UV-Vis spectral analyses confirm the AgNPs peak at 456 nm. Larvicidal activity of AgNPs exhibited significant toxic effects on *Cx. quinquefasciatus*. In-vitro antioxidant study displayed a significant activity on scavenging of free radicals activity. The anti-cancer potential of AgNPs was showed dose dependent activity and IC<sub>50</sub> value of 33.05 μg/mL against colon cancer cell line. Antibacterial activity of *Ps*-AgNPs of tested microbes showed good activity at higher concentrations. Overall, the outcome of the study clearly stated the *Ps*-AgNPs act as simple, eco-friendly and low cost approach could be useful for the control of vector bone diseases and biomedical applications.

#### Declaration of Competing Interest

The authors declare that they have no known competing financial interests or personal relationships that could have appeared to influence the work reported in this paper.

#### Acknowledgement

The authors Acknowledge to Periyar University, Salem to providing University Research Fellowship (Ref. No. PU/AD-3/URF/2016). The authors also thank to Department of Botany, School of Life Sciences, Periyar University, Salem, Tamil Nadu-636 011, India, for providing infrastructural facility. The authors extend their appreciation to the Researchers supporting project number (RSP2022R470) King Saud University, Riyadh, Saudi Arabia.

#### References

Abbott, W. S., 1925. A method of computing the effectiveness of an insecticide. *J. Econ. Entomol.* 18, 265–267.

Aritonang, H.F., Koleangan, H., Wuntu, A.D., 2019. Synthesis of silver nanoparticles using aqueous extract of medicinal plants' (Impatiens balsamina and Lantana camara) fresh leaves and analysis of antimicrobial activity. *Int. J. Microbiol.* 2019, 1–8.

Alwhibi, M.S., Soliman, D.A., al khalidy, H., Alonzaian, A., Abdulhaq Marraiki, N., El-Zaidy, M., AlSubeie, M.S., 2020. Green biosynthesis of silver nanoparticle using *Commiphora myrrh* extract and evaluation of their antimicrobial activity and colon cancer cells viability. *J. King Saud Univ.-Sci.* 32 (8), 3372–3379.

Anonymous, (1996). Pharmacopoeia of India (The Indian Pharmacopoeia), 3<sup>rd</sup>Edn., Govt. of India, New Delhi, Ministry of Health and Family Welfare.

Ashwini, U., Asha, S., 2017. Larvicidal activity of natural products against mosquito species. *Int. J. Chem. Technol. Res.* 10, 875–878.

Balaraman, P., Balasubramanian, B., Kaliannan, D., Durai, M., Kamyab, H., Park, S., Chelliapan, S., Lee, C.T., Maluven, V., Maruthupandian, A., 2020. Phyco-synthesis of silver nanoparticles mediated from marine algae *Sargassum myricocystum* and its potential biological and environmental applications. *Waste Biomass Valor.* 11 (10), 5255–5271.

Bharathi, D., Bhuvaneshwari, V., 2019. Evaluation of the cytotoxic and antioxidant activity of phyto-synthesized silver nanoparticles using *Cassia angustifolia* flowers. *BioNano Sci.* 9 (1), 155–163.

Bharathi, D., Diviya Josebin, M., Vasantharaj, S., Bhuvaneshwari, V., 2018. Biosynthesis of silver nanoparticles using stem bark extracts of *Diospyros montana* and their antioxidant and antibacterial activities. *J. Nanostruct. Chem.* 8 (1), 83–92.

Bhat, M., Chakraborty, B., Kumar, R.S., Almansour, A.I., Arumugam, N., Kotresha, D., Pallavi, S.S., Dhanyakumara, S.B., Shashiraj, K.N., Nayaka, S., 2021. Biogenic synthesis, characterization and antimicrobial activity of *Ixora brachypoda* (DC) leaf extract mediated silver nanoparticles. *J. King Saud Univ.-Sci.* 33 (2), 101296. <https://doi.org/10.1016/j.jksus.2020.101296>.

Chakraborty, B., Kumar, R.S., Almansour, A.I., Kotresha, D., Rudrappa, M., Pallavi, S.S., Nayaka, S., 2021. Evaluation of antioxidant, antimicrobial and antiproliferative activity of silver nanoparticles derived from *Galphimia glauca* leaf extract. *J. King Saud Univ.-Sci.*, 101660.

Chunche Gowda, U.A., Shivaram, A.B., Mahadevamurthy, M., Ramachandrapa, L.T., Lalitha, S.G., Krishnappa, H.K.N., Ramachandrapa, N.S., 2020. Biosynthesis of zinc oxide nanoparticles using leaf extract of *Passiflora subpeltata*: characterization and antibacterial activity against *Escherichia coli* isolated from poultry faces. *J. Cluster Sci.*, 1–10.

Dehghanizade, S., Arasteh, J., Mirzaie, A., 2018. Green synthesis of silver nanoparticles using *Anthemisa tropatana* extract: characterization and in vitro biological activities. *Artif. Cells Nanomed. Biotechnol.* 46 (1), 160–168.

Divya, M., Vaseeharan, B., Abinaya, M., Vijayakumar, S., Govindarajan, M., Alharbi, N. S., Kadaikunnan, S., Khaled, J.M., Benelli, G., 2018. Biopolymer gelatin-coated zinc oxide nanoparticles showed high antibacterial, antibiofilm and anti-angiogenic activity. *J. Photochem. Photobiol., B* 178, 211–218.

Fafal, T., Taştan, P., Tüzün, B.S., Ozyazici, M., Kivcak, B., 2017. Synthesis, characterization and studies on antioxidant activity of silver nanoparticles using *Asphodelus aestivus* Brot. aerial part extract. *S. Afr. J. Bot.* 112, 346–353.

Gul, H., Khan, F.S., Afzal, U., Batool, S., Saddick, S., Awais, M., Irum, S., Malik, M.Y., Ijaz Khan, M., Alhazmi, A., Khan, S.U., 2021a. *Rumex hastatus* derived silver nanoparticles development and their potential applications as hepatic-protection agent along with antimicrobial activity. *J. King Saud Univ.-Sci.* 33 (7), 101587. <https://doi.org/10.1016/j.jksus.2021.101587>.

Gul, H., Khan, F.S., Afzal, U., Batool, S., Saddick, S., Awais, M., Khan, S.U., 2021b. *Rumex hastatus* derived silver nanoparticles development and their potential applications as hepatic-protection agent along with antimicrobial activity. *J. King Saud Univ.-Sci.* 33, 101587.

Guntur, S.R., Kumar, N.S., Hegde, M.M., Dirisala, V.R., 2018. In vitro studies of the antimicrobial and free-radical scavenging potentials of silver nanoparticles biosynthesized from the extract of *Desmostachya bipinnata*. *Anal. Chem. Insights* 13. <https://doi.org/10.1177/1177390118782877>.

Huong, V.T.L., Nguyen, N.T., 2021. Green synthesis, characterization and antibacterial activity of silver nanoparticles using *Sapindus mukorossi* fruit pericarp extract. *Mater. Today.* Proc. 42, 88–93.

Kasi, S.D., Ramasamy, J.M., Nagaraj, D., Santiyagu, V., Ponraj, J.S., 2021. Biogenic synthesis of copper oxide nanoparticles using leaf extracts of *Cissus quadrangularis* and *Piper betle* and its antibacterial effects. *Micro Nano Lett.* 16 (8), 419–424.

Khandel, P., Yadav, R.K., Soni, D.K., Kanwar, L., Shahi, S.K., 2018. Biogenesis of metal nanoparticles and their pharmacological applications: present status and application prospects. *J. Nanostruct. Chem.* 8, 217–254.

Kora, A.J., Manjusha, R., Arunachalam, J., 2009. Superior bactericidal activity of SDS capped silver nanoparticles: synthesis and characterization. *Mater. Sci. Eng., C* 29, 2104–2109.

Loganathan, S., Selvam, K., Sivasakthi, V., Prakash, P., Yamuna, M., Lalitha, K., Shivakumar, M.S., Senthil Nathan, S., 2021a. Phytochemical and pharmacological evaluation of methanolic extract of *Knoxia sumatrensis* leaves. *J. Herbs Spices Med Plants* 27 (2), 200–217.

- Loganathan, S., Shivakumar, M.S., Karthi, S., Nathan, S.S., Selvam, K., 2021b. Metal oxide nanoparticle synthesis (ZnO-NPs) of *Knoxia sumatrensis* (Retz.) DC. Aqueous leaf extract and its evaluation of their antioxidant, anti-proliferative and larvicidal activities. *Toxicol. Rep.* 8, 64–72.
- Marambio-Jones, C., Hoek, E.M.V., 2010. A review of the antibacterial effects of silver nanomaterials and potential implications for human health and the environment. *J. Nanopart. Res.* 12 (5), 1531–1551.
- Mohanta, Y.K., Panda, S.K., Jayabalan, R., Sharma, N., Bastia, A.K., Mohanta, T.K., 2017. Antimicrobial, antioxidant and cytotoxic activity of silver nanoparticles synthesized by leaf extract of *Erythrina suberosa* (Roxb.). *Front. Mol. Biosci.* 4, 14.
- Mosmann, T., 1983. Rapid colorimetric assay for cellular growth and survival: application to proliferation and cytotoxicity assays. *J. Immunol. Methods* 65 (1–2), 55–63.
- Mtambo, S.E., Krishna, S.B.N., Sershen, Govender, P., 2019. Physico-chemical, antimicrobial and anticancer properties of silver nanoparticles synthesised from organ-specific extracts of *Bidens pilosa* L. *S. Afr. J. Bot.* 126, 196–206.
- Nahar, K., Aziz, S., Bashar, M., Haque, M., Al-Reza, S.M., 2020. Synthesis and characterization of Silver nanoparticles from *Cinnamomum tamala* leaf extract and its antibacterial potential. *Int. J. Nano Dimens.* 11, 88–98.
- Patra, J.K., Das, G., Fraceto, L.F., Campos, E.V.R., Rodriguez-Torres, M.D.P., Acosta-Torres, L.S., Diaz-Torres, L.A., Grillo, R., Swamy, M.K., Sharma, S., Habtemariam, S., Shin, H.-S., 2018. Nano based drug delivery systems: recent developments and future prospects. *J. Nanobiotechnol.* 16 (1). <https://doi.org/10.1186/s12951-018-0392-8>.
- Patra, J.K., Das, G., Shin, H.S., 2019. Facile green biosynthesis of silver nanoparticles using *Pisum sativum* L. outer peel aqueous extract and its antidiabetic, cytotoxicity, antioxidant, and antibacterial activity. *Int. J. Nanomed.* 14, 6679.
- Rajkumar, R., Shivakumar, M.S., Senthil Nathan, S., Selvam, K., 2018. Pharmacological and larvicidal potential of green synthesized silver nanoparticles using *Carmona retusa* (Vahl) Masam leaf extract. *J. Cluster Sci.* 29 (6), 1243–1253.
- Rathnakumar, S.S., Noluthando, K., Kulandaiswamy, A.J., Rayappan, J.B.B., Kasinathan, K., Kennedy, J., Maaza, M., 2019. Stalling behaviour of chloride ions: a non-enzymatic electrochemical detection of  $\alpha$ -Endosulfan using CuO interface. *Sens. Actuators, B* 293, 100–106.
- Roshni, K., Younis, M., Ilakkiyapavai, D., Basavaraju, P., Puthamohan, V.M., 2018. Anticancer activity of biosynthesized silver nanoparticles using *Murraya koenigii* leaf extract against HT-29 colon cancer cell line. *Sci. World J. Cancer Sci. Ther.* 10, 72–75.
- Senthil-Nathan, S., 2013. Physiological and biochemical effect of neem and other Meliaceae plants secondary metabolites against Lepidopteran insects. *Front. Physiol.* 4, 359.
- Senthil-Nathan, S., 2015. A review of biopesticides and their mode of action against insect pests. In: Thangavel, P., Sridevi, G. (Eds.), *Environmental Sustainability*. Springer India, New Delhi, pp. 49–63. [https://doi.org/10.1007/978-81-322-2056-5\\_3](https://doi.org/10.1007/978-81-322-2056-5_3).
- Senthil-Nathan, S., 2020. A review of resistance mechanisms of synthetic insecticides and botanicals, phytochemicals and essential oils as alternative larvicidal agents against mosquitoes. *Front. Physiol.* 10, 1591.
- Sk, I., Khan, M.A., Haque, A., Ghosh, S., Roy, D., Homechudhuri, S., Alam, M.A., 2020. Synthesis of gold and silver nanoparticles using *Malva verticillata* leaves extract: Study of gold nanoparticles catalysed reduction of nitro-Schiff bases and antibacterial activities of silver nanoparticles. *Curr. Opin. Green Sustainable Chem.* 3, 100006. <https://doi.org/10.1016/j.crgsc.2020.05.003>.
- Sowndarya, P., Ramkumar, G., Shivakumar, M.S., 2017. Green synthesis of selenium nanoparticles conjugated *Clausena dentata* plant leaf extract and their insecticidal potential against mosquito vectors. *Artif. Cells Nanomed. Biotechnol.* 45 (8), 1490–1495.
- Sultana, N., Raul, P.K., Goswami, D., Das, D., Islam, S., Tyagi, V., Raju, P.S., 2020. Bio-nanoparticle assembly: a potent on-site biolarvicidal agent against mosquito vectors. *RSC Adv.* 10, 9356–9368.
- Thandapani, K., Kathiravan, M., Namasivayam, E., Padiksan, I.A., Natesan, G., Tiwari, M., Perumal, V., 2018. Enhanced larvicidal, antibacterial, and photocatalytic efficacy of TiO<sub>2</sub> nanohybrids green synthesized using the aqueous leaf extract of *Parthenium hysterophorus*. *Environ. Sci. Pollut. Res.* 25, 10328–10339.
- Vijayaraghavan, K., Nalini, S.K., Prakash, N.U., Madhankumar, D., 2012. Biomimetic synthesis of silver nanoparticles by aqueous extract of *Syzygium aromaticum*. *Mater. Lett.* 75, 33–35.
- World Health Organization (WHO) (2005). Geneva. [www.WHO/CDS/WHOPES/GCDPP/13](http://www.WHO/CDS/WHOPES/GCDPP/13).